SHEAR BOLTED CONNECTIONS: NUMERICAL MODEL FOR A DUCTILE COMPONENT, THE PLATE-BOLT IN BEARING

J. Henriques*, L. Ly, J.-P. Jaspart** and L. Simões da Silva***

* ISISE, Departamento de Engenharia Civil, Faculdade Ciências e Tecnologia, Universidade de Coimbra
e-mails: jagh@dec.uc.pt, luisss@dec.uc.pt

** MS²F, ArGEnCo, Faculté de Sciences Appliquées, Université de Liège
e-mail: dplam.ly@ulg.ac.be, Jean-Pierre.Jaspart@ulg.ac.be

Keywords: Shear, Connection, Component, Bearing, Plastic.

Abstract. In order to achieve a full plastic distribution of forces in a shear bolted connection, ductility is required to the steel plate and to the plate-bolt contact zone in the firstly loaded bolt rows. Knowing that bolts present a brittle behavior, deformation capacity has to be obtained from ductile components as the plate-bolt in bearing. In the present paper a numerical model is proposed to evaluate the plate-bolt in bearing component. The main objective is not only to achieve it elastically but to obtain a good approximation of the post-elastic response. The proposed model has been successfully validated by experimental tests on shear bolted connections performed at the Delft University of Technology and at the University of Ljubljana. The EC3 Part 1.8 [1] approach, to evaluate resistance and initial stiffness of the plate–bolt in bearing component, is included in the comparison and discussion of results.

1 INTRODUCTION

In shear bolted connections forces are transferred from one plate to another (others) by plate-to-bolt contact. Neglecting the small friction developed between plates and the negligible bending of the bolt, four sources of resistance and deformation modes should be considered: bearing of the plate and/or bolt; shear in the plates; tension in the plates; shear in the bolt shanks. In these types of connections, the load to be transferred between the plates is distributed non-uniformly amongst the bolt-rows (Figure 1). In [2], Ju *et al* showed that in the nonlinear range the maximum load achieved by the connection is almost linearly proportional to the number of bolts in the connection. According to [1], a full plastic distribution of forces can be assumed as long as the connection length is limited. Pietrapetrosa *el al* [3] studied fitted bolted connections and showed that, inside the limits given by the code and by practical guidance, sufficient ductility to achieve a full plastic distribution of internal forces is available. On the other hand, Wald *et al* [4] verified that if imperfections (misalignment of bolts) are considered, failure could be first attained in the extreme bolts and therefore a full plastic resistance was not reached. The presence of imperfections requires therefore higher deformation capacity from the connection components. Knowing that the bolt has a brittle behavior, ductility has to be obtained from the plate-bolt in bearing component in order to achieve a full plastic resistance, as observed in [5]

In EC3 Part 1.8 [1] the bearing resistance and the bearing stiffness may be determined using the proposed design functions. However, these functions are mainly directed to mild steel and to connections with normal round holes. So, in this paper, the calibration of a numerical model to study the plate-bolt in bearing component, which can be later used to extend the actual knowledge to new common practices (connections with High Strength Steel, oversized or slotted holes, etc), is presented. Tests made on shear bolted connections at the University of Ljubljana and at the Delft University of Technology are used to

validate the numerical model. In the absence of experimental work which addressed only the phenomenon of bearing, the validation of the numerical model is done using experimental work on bolted shear connections. The use of this type of tests influences the numerical model as bearing is not isolated, so that other phenomena have to be taken into account.

The 3D finite element model is compared with the experiments in terms of stiffness, strength and ductility allowing evaluating and commenting the reliability of the developed model. Additionally, a comparison with EC3 Part 1.8 [1] recommendations is presented.
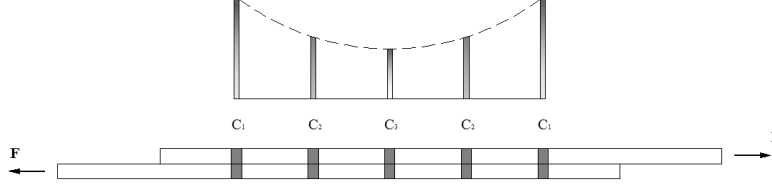

Figure 1 – Elastic distribution of forces in shear bolted connections.

2 CODE APPROACH

The plate-bolt in bearing is a complex component as its behavior is influenced by phenomena such as: shear forces developed in the plate, net section deformability, contact problems (bolt/plate), friction and confinement between plates. So, many different parameters as bolt and hole diameter (d and d_0), plate thickness (t), edge and end distances (e_2 and e_1), spacing (p_1 and p_2), bolt and plate material (grade) should be taken into account. Using reduction factors, the design bearing resistance defined in EC3 Part 1.8 [1] considers all the referred geometrical and material parameters and is expressed as:

$$F_{b,Rd} = \frac{\alpha_b k_1 f_u dt}{\gamma_{M2}} \tag{1}$$

where: the reduction factors α_b and k_1 introduce the additional influence of geometric and material properties, as defined in EC3 Part 1.8 [1].

The initial stiffness for the plate-bolt in bearing component may be obtained from EC3 Part 1.8 [1] stiffness coefficient.

$$S_{p,b} = 12 k_b k_t df_u \tag{2}$$

where: the factors k_b and k_t take into account the geometrical properties as expressed in EC3 Part 1.8 [1].

The ultimate deformation of plate/bolt in bearing is based on the mechanical properties of mild steel; an expression has been derived from experimental tests by Jaspart [6]. No recommendation is found in the EC3 Part 1.8 [1].

$$\delta_{u,p} = 11 \frac{F_{b,Rd}}{S_{p,b}} \tag{3}$$

3 EXPERIMENTAL DATA

In the Delft University of Technology [8] and in the University of Ljubljana [9], shear bolted connections, with one and two bolts, made of high strength steel (S690) were tested. In the present paper only one bolt joints are used for numerical validation. Figure 2 illustrates the specimens general configuration. Table 1 and Table 2 present the relevant data of the used specimens.
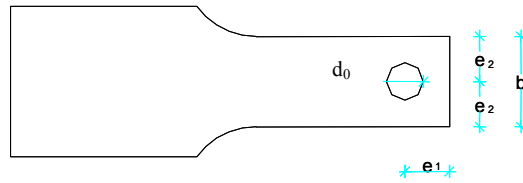
Figure 2 – Specimens configuration.

Table 1 – Data for the specimens tested at Delft University.

Test ID	Plate							Bolt		
	e_1/d_0	e_2/d_0	b [mm]	t [mm]	A_{gross} [mm]	A_{net} [mm]	Class	d [mm]	d_0 [mm]	Class
A1210	1,2	1,0	52	10	520	260	S690	24	26	10.9
A1212	1,2	1,2	62,4	10	624	364	S690	24	26	10.9
A1215	1,2	1,5	78	10	780	520	S690	24	26	10.9
A2020	2,0	2,0	104	10	1040	780	S690	24	26	10.9

Table 2 – Data of the specimens tested at Ljubljana University.

Test ID	Plate							Bolt		
	e_1/d_0	e_2/d_0	b [mm]	t [mm]	A_{gross} [mm]	A_{net} [mm]	Class	d [mm]	d_0 [mm]	Class
B110	1,2	1,5	90	10	900	600	S690	27	30	10.9
B113	2,5	1,5	90	10	900	600	S690	27	30	10.9
B117	1,5	1,5	90	10	900	600	S690	27	30	10.9

4 NUMERICAL MODEL

4.1 General description

The numerical tool used is LAGAMINE [7] which is a software developed at ArGenCo Department at the University of Liège. The basic model to study the bearing component consists in a plate with a hole which is pushed in the longitudinal direction by a rigid element (bolt). The plate is fixed in the opposite end direction. Figure 3-a) shows an illustration of the idealized basic model. Because in the experiments double overlap bolted connections were tested, numerical results had to be extrapolated for comparison. Profiting from the symmetry of the problem, only half of the width and of the thickness has been modeled and additional boundary conditions are considered accordingly. Because of the concentration of stresses expected around the hole, especially in the bearing zone, the mesh refinement is higher in this region, as illustrated in Figure 3-b).

The plate is modeled using the 3D volume elements (BLW3D) available in LAGAMINE [7]. This is a 8 node element with 1 Gauss integration point. For the bolt, two different modeling have been analyzed. Initially, the bolt has been modeled as a rigid element, no deformation being considered. Subsequently, a deformable bolt is assumed and the same volume elements and symmetry simplifications have been used. To model the contact, the plane elements (CIF3D), available for three-dimensional mechanical contact problems, have been used. The CFI3D is composed by 4 nodes and 4 Gauss integration points.

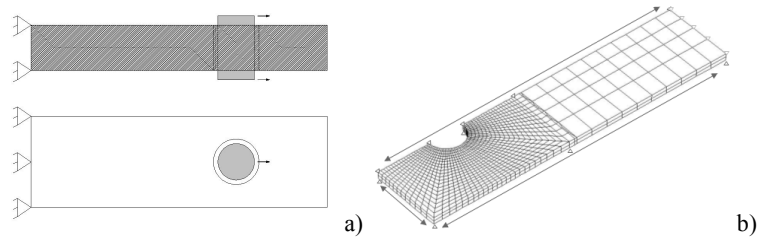a)   b)

Figure 3 – Idealized model.

4.2 Constitutive law

In order to simulate ductility the usual characterization of the steel behavior has a limited field of application and therefore a more accurate characterization is required. The usual (nominal) stress-strain (σ_n-ε_n) curve is derived considering conservation of the cross-section which is reflected in non-negligible false stress when relevant plastic deformations begin. The standard procedure of uniaxial tension tests disregards the updating of the cross-section. Consequently, the true stress (σ_t) can be obtained applying a correction on the nominal value (F_i/A_0). Regarding the strain, logarithmic strain is known as the true strain (ε_t), and has been used here. Thus, the true stress and the true strain may be determined as follows.

$$\sigma_t = \frac{F_i}{A_0 \left(\frac{1}{\sqrt{\left(1 + \varepsilon_{n,x}^p\right)}} - \upsilon \varepsilon_{n,x}^e \right)^2} \tag{4}$$

$$\varepsilon_t = \ln\left(1 + \varepsilon_n\right) \tag{5}$$

where: F_i is the force applied at each load step; A_0 is the initial cross-section; $\varepsilon_{n,x}^p$ and $\varepsilon_{n,x}^e$ are the nominal plastic and elastic strains in the longitudinal direction; υ is the Poisson's ratio.

The presented formulae are only applicable up to the beginning of necking. With necking the element loses its uniformity and a local striction begins. Consequently, in the nominal stress-strain curve, a decrease of the stress is observed; however this loss of capacity is not real. With Kato (1990) [10] mathematical expression, the constitutive law can be corrected beyond necking. However, this requires a correct determination of the strain, which is often not possible with standard procedure of material characterization tests.

4.3 Calibration of the numerical model

- Constitutive law: In Figure 4-a) are represented the three analyzed models: nominal; correction neglecting the necking phenomenon; and correction considering a plateau. In Figure 4-b), using the test specimen A2020 the obtained results are presented. Clearly, the nominal stress-strain curve is insufficient to reproduce the complete force-deformation curve observed in the tests. As reported, the use of the true stress and the true train gives a good approximation to experimental results. The neglect of the necking effect can be seen through the cure A2020 corrected-1 with a small loss of load capacity, compared to experimental results; and then using correction with plateau after necking allows obtaining better results.

- Bolt model: Two types of bolt modeling have been analyzed: rigid bolt; and deformable bolt. Figure 5-a) compares the obtained force-deformation curves. No significant variation is noticed. Figure 5-b) illustrates the stress distribution for the points represented in the curve. Again, no relevant difference is noticed.

- <u>Confinement effect</u>: Three models have been analyzed: i) confinement modeled by constraining, at the top surface, part of the nodes (adjacent to bolt-plate contact) in the transversal direction; ii) confinement considered by modeling part of the outer plate; iii) model without confinement. In Figure 6 the comparison with experimental results clearly shows that the confinement should be considered. Comparing the two types of confinement it can be verified that modeling the outer plate provides relatively higher resistance. However, this modeling implies the calibration of the friction coefficient.
- <u>Friction coefficient</u>: In all the models presented so far the usual value of 0.3 has been considered. In the literature, some values have been found for an approximate value of the friction coefficient to use for contact surfaces clamped by bolts; the values presented for contact surfaces steel on steel vary from 0.15 to 0.25. In Figure 7, the comparison between the different values taken for the friction coefficient is shown. The results show that the value of 0.20 fits better when compared to experimental results.
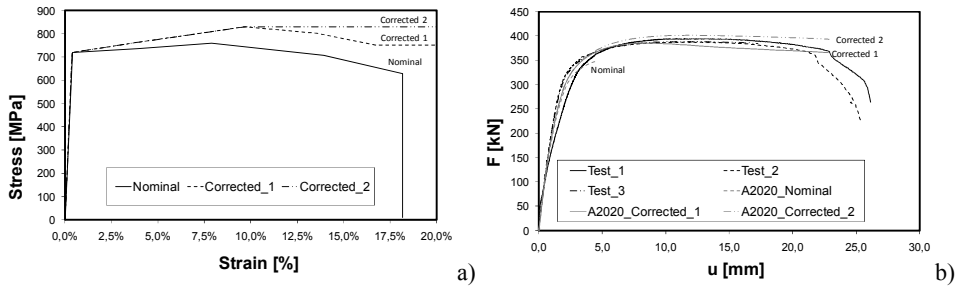
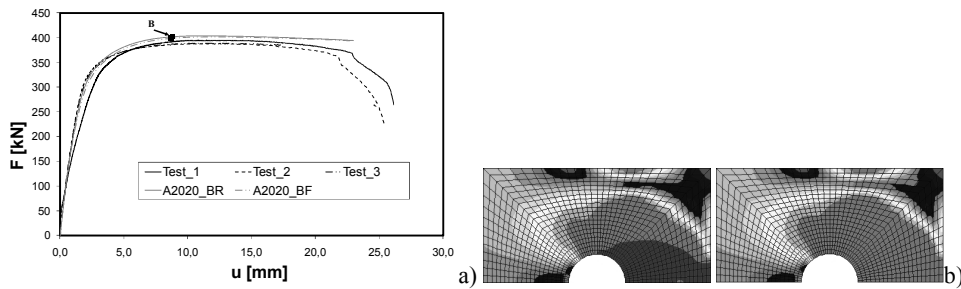Figure 4 – a) Different constitutive laws analyzed; b) Comparison of the constitutive laws influence.

Figure 5 – a) Comparison between the rigid and the flexible bolt modeling; b) left – stress distribution for rigid bolt modeling and right – stress distribution for flexible bolt modeling for load step represented by point B.
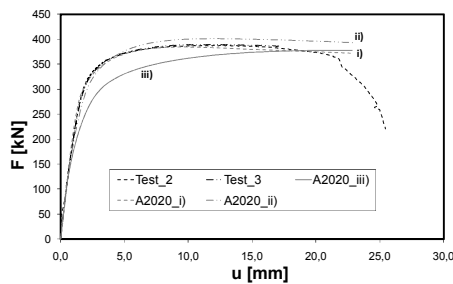
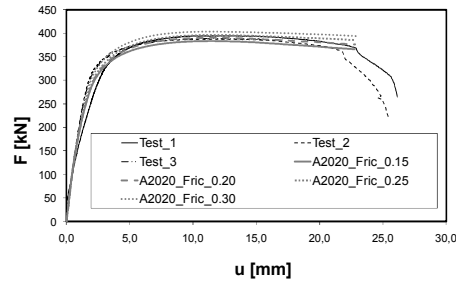Figure 6 – Comparison of the models to study the confinement effect.

Figure 7 – Comparison of results using different friction coefficient.

Finally, as a conclusion of the parametric study, the numerical calculations presented hereafter consider: constitutive law corrected and necking effect considered assuming a plateau; bolt is modeled as rigid; outer plate is modeled in order to introduce the confinement effect; and the friction coefficient has been taken equal to 0.2.

5 ANALYSIS OF RESULTS

5.1 Comparison with experimental tests

In this paper, only two specimens are used to compare results. Additional results may be found in [11]. Figure 8-a) presents the load-displacement curves for test specimen A1210 and the corresponding numerical model. This specimen failed by net-cross section failure. From the load displacement curves one can observe that the numerical model has a good accuracy. Initial stiffness and resistance are well approximated. In Figure 8-b) and c) the test failure pattern and final deformation of the numerical model may be compared. The numerical model achieved a correct deformation shape when compared with the experimental failure configuration.

Figure 9-a) presents the load displacement curves for test specimen B113 and for the corresponding numerical model. This specimen presented a bearing failure. In Figure 9-b) and c), test failure pattern and final deformation of the numerical model are illustrated. Good approximation is observed between the numerical calculation and the experimental tests.
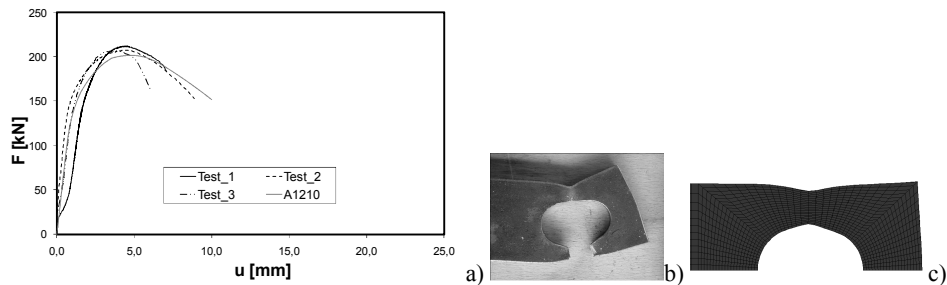

Figure 8 – Comparison of results for A1210 specimen: a) load-displacement curve; b) test failure configuration; c) numerical model final deformed configuration.
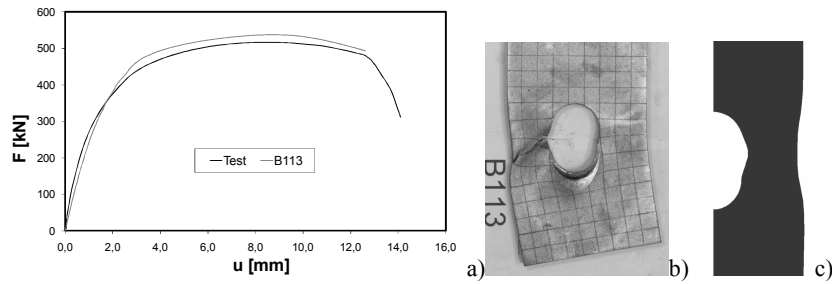
Figure 9 – Comparison of results for B113 specimen: a) load-displacement curve; b) test failure configuration; c) numerical model final configuration.

5.2 Comparison with code approach

For comparison, specimens A1212 and A1215 are used. More results may be found in [11]. Results are presented in Figure 10 and Figure 11. For comparison of resistance and initial stiffness, the used numerical calculations correspond to the pure bearing behavior of the tested plate, no extrapolation is therefore required and no confinement was considered. In order to compare the ultimate deformation using equation (3) with experimental results, an extrapolation to double overlap connections is done.
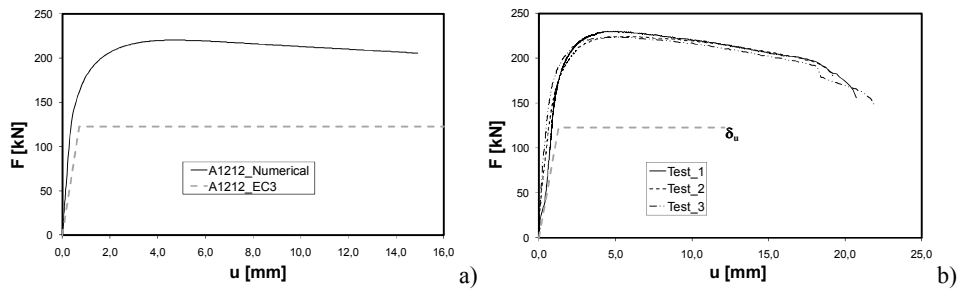

Figure 10 – Comparison of results using A1212 specimen: a) numerical model vs EC3 Part 1.8 [1] approach; b) ultimate deformation according to (3) vs experimental tests.
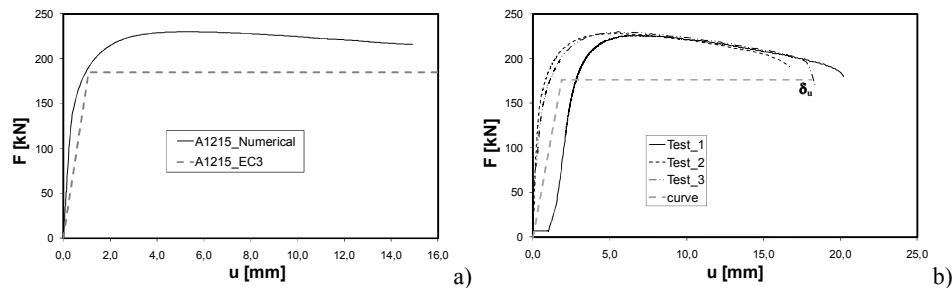

Figure 11 – Comparison of results using A1215 specimen: a) numerical model vs EC3 Part 1.8 [1] approach; b) ultimate deformation according to (3) vs experimental tests.

In terms of resistance, the code evaluation for specimen A1212 is not in line with the numerical model; there is a difference of up to 44%. This difference is justified by two aspects: first, a lower value of ultimate resistance (f_u) is assumed by the code for calculation according to (1) when compared with the real one; secondly, and most relevant, the reduction factors defined by the Eurocode are not appropriate

for High Strength Steel. Parameter e_2 penalizes excessively the bearing resistance. For the models A1215, the deviation in the results (resistance) is much lower, about 20%. Here, the lower ultimate resistance of the steel used by code approach should be the main explanation. For the initial stiffness, all models present more a less the same differences. Finally, the estimation of the ultimate deformation (δ_u) using expression (3) presents, for model A1215, very close results in comparison to experiments. On the other hand, great difference is noticed for model A1212 which should be justified by the fact that expression (3) is based on the resistance determined by the code approach; and this was shown not to be appropriate when dealing with low edge distances in plates made of High Strength Steel.

6 CONCLUSIONS

In the present paper a numerical model to evaluate the plate/bolt in bearing component has been proposed. The experimental tests used for validation considered double overlap connections. Consequently, phenomena which are not directly related to the bearing deformation have been introduced in the model, as confinement and friction effects. The model was successfully validated by the experiments. Net-section failure was also simulated with success. Therefore, the suitability of the numerical model is assured. EC 3 part 1.8 [1] approach has been compared with the numerical simulation; it has been observed that in the case of High Strength steel some improvement should be brought to the expressions enabling to determine the resistance and the initial stiffness. The influence of edge distance as predicted by the code for mild steel has a limited application to HSS.

REFERENCES

[1] CEN European Committee for Standardization, *Eurocode 3: Design of steel structures – Part 1-8: Design of joints*, EN 1993-1-8, Brussels, Belgium, 2005.

[2] Ju S.-H, Fan C.-Y. and Wu G. H., *Three-dimensional finite elements of steel bolted connections*, Engineering Structures 26, 403-413, 2003.

[3] Pietrapertosa C., Piraprez E. and Jaspart J.P., *Ductility requirements in shear bolted connections*, ECCS/AISC Workshop: Connections in steel structures V: Behaviour, Strength and Design, Amsterdam, The Netherlands, June 3-4, pp. 335-345, 2004.

[4] Wald F., Sokol Z., Moal M., Mazura V. and Muzeau J. P. , *Stiffness of cover plate connections with slotted holes*, Eurosteel: Third European conference on Steel Structures, Coimbra, Portugal, pp. 1007-1016, 2002.

[5] Henriques J., Jaspart J.-P. and Simões da Silva L., *Ductility requirements for the design of bolted shear connections*, AISC ECCS Workshop, Chicago, 2008.

[6] Jaspart J.-P., *Étude de la semi-rigidité des nœuds poutre-colonne et son influence sur la resistance des ossatures en acier*, Doctor Thesis, Department MSM, University Liège, Belgium, 1991.

[7] LAGAMINE code, Finite Element Software, ArGEnCO Department, Liège University, Belgium.

[8] Freitas S. T., *Experimental research project on bolted connections in bearing for high strength steel*, Final report of the framework of the Socrates-Erasmus program, June 2005.

[9] Moze P., Beg, D. and Lopatic J., *Ductility and Strength of bolted connections made of high strength steel*, International conference in metal structures "Steel – A new and traditional material for buildings", Poiana Brasov, Romania, Sptember 20-22, pp. 323-330, 2006.

[10] Kato B., *Tension testing of metallic structural materials for determining stress-strain relations under monotonic and uniaxial tensile loading*, Rilem draft recommendation, TC 83 – CUS Fundamental Mechanical Properties of Metals, 1990, 23, 35-46, 1990.

[11] Henriques J., *Ductility requirements in shear bolted connections*, Master Thesis, Civil Engineering Department, University of Coimbra, Portugal, 2008.